

# BEAM PROFILE MONITOR FOR SLOW EXTRACTED BEAM USING MULTI-LAYERED GRAPHENE AT J-PARC

Y. Hashimoto<sup>†</sup>, Y. Hori, R. Muto, M. Tomizawa, T. Toyama, M. Uota, KEK/J-PARC, Tokai, Japan  
 M. Murakami, K. Murashima, M. Tachibana, A. Tatami, KANEKA CORPORATION, Osaka, Japan  
 M. Endo, H. Sakai, Mitsubishi Electric System & Service Co., Ltd., Tsukuba, Japan

## Abstract

Extracted-beam profiles were measured in slow extraction at J-PARC using secondary electrons emitted from a ribbon-target array made of multi-layered graphene, in real-time during a spill time of 2 seconds. The target array consisted of 20 ribbons with a width of 1 mm, a pitch of 2 mm, and a thickness of 1.1  $\mu\text{m}$ . The secondary-electron current at each channel was measured using current amplifiers with a sensitivity of more than 1 pA. The features of this instrument and a recent beam study with a 51 kW extracted beams are discussed.

## INTRODUCTION

Graphite ribbons with a thickness of 2 to 3  $\mu\text{m}$  have been utilized for high-intensity beam as the target for emitting secondary electrons in profile measurement at the beam transport line (3-50 BT) in the J-PARC Main Ring (MR) [1]. This monitor has been called a multi-ribbon beam profile monitor (MRPM). The use of a thinner uniform graphite foil has the advantages of reduced beam loss, reduced heat generation, and a high heat resistance of the graphite foil. The following points are noted regarding the durability of MRPM. The maximum beam intensity in the measurement at 3-50 BT was  $3.9 \times 10^{13}$  p/bunch which corresponded to 1 MW beam in MR. In addition, one MRPM was used in the slow extraction (SX) beamline to continuously measure the profile of 30 GeV (resent beam power was 51 kW [2]) from the first SX beam in 2009. The total number of protons passed through was  $1.2 \times 10^{20}$  or more.

As for the target materials, Kaneka facilitates the production of excellent foils for J-PARC use based on the research results of multi-graphene fabrication. The foil has a reduced thickness of 1.0 -1.2  $\mu\text{m}$  with high uniformity over its entire surface [3]. Evolved MRPM using this multi-graphene target set in two places on SX section. The first SX-MRPM was installed in 2015 and the second in 2017.

## SX DEVICES AND BEAM

Figure 1 shows the layout of SX section. The SX components are the upper ESS1, 2 (electrostatic septum) and the lower SMS1, 2, 3 (septum magnet). The SX beam is led to the hadron beamline. The entrance and exit at these devices are the positions where the remarkable beam characteristics can be measured. SX-MRPM #82 and #83 were installed at the entrance of SMS1 and SMS2, respectively. The graphite MRPM, used since 2009, is located at the hadron beamline. The following describes SX-MRPM #82.

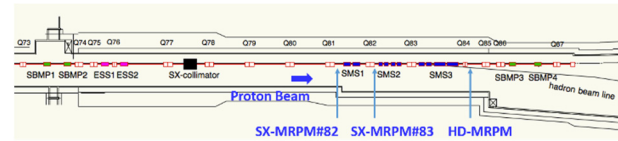


Figure 1: Layout of Slow Extraction Section in MR.

Figure 2 shows the simulation result of the SX beam 30 GeV at the entrance of SMS1. The emittance of the injection beam was assumed to be  $81 \pi$  mm. mrad. For the X and Y cross-sections, the injection beam ( $3\sigma$ ) is represented by a red circle, the extraction beam is shown in black, and the beams up to 3 turns ago are represented in other colors. The dimensions of the extraction beam were approximately X 10 mm, Y 22 mm. The turn separation of the circulating beam and the SX is approximately 3 mm. It was necessarily to design the target frame to avoid hitting the injection beam. The distance between the extraction beam and the injection beam was approximately 10 mm. The beam measurement at extraction can be performed without interference due to the injection beam by arranging the target frame with the inner dimension of 70 mm in the Y direction as shown in the figure.

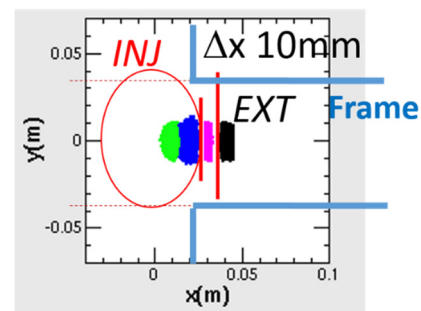


Figure 2: 30GeV Extracted-Beam Simulation.

## MULTI-GRAPHENE RIBBON TARGET

Figure 3 (a) shows the multi-graphene ribbon targets for horizontal profile measurement. The electrode wiring pattern of AgPt was fired on a 2 mm-thick C-shaped ceramic frame. In design, the pitch of the ribbon was 2 mm, the width was 1 mm, the thickness was 1.1  $\mu\text{m}$ , and channel number of 20 was configured. The measured results of the ribbon width made by laser cut was 0.998 mm in average and 0.4 % in standard deviation. The target assembly is shown in Figure 3 (b). The multi-graphene targets A to E were arranged with a spacing of 6 mm. Target B is a ribbon for horizontal measurement (Fig. 3(a)), whereas target D is a ribbon tilted at 15 degrees so that the indication of the

<sup>†</sup> yoshinori.hashimoto@kek.jp.

Content from this work may be used under the terms of the CC BY 3.0 licence (© 2019). Any distribution of this work must maintain attribution to the author(s), title of the work, publisher, and DOI

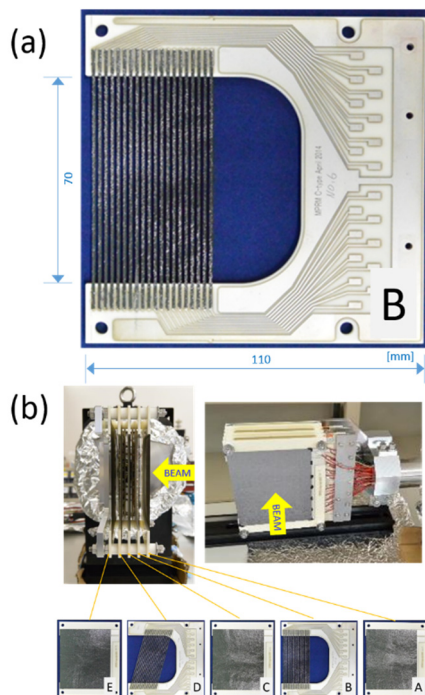


Figure 3: (a) Multi-Graphene ribbon target, (b) Target assembly.

vertical component could be seen. The targets A, C and E have the function of capturing secondary electrons generated by the ribbon via the application of a positive voltage. The signal in the tunnel is sent to a local control room 170 m away using a shielded 1.5 Dia.-34ch collective coaxial cable.

## SIGNAL PROCESSING

### I/V Amplifier

In the SX of several 10-kW classes, several  $\mu\text{A}$  beams were extracted over approximately 2 seconds of spill time. Given that the secondary electron (SE) emission efficiency with a proton beam of GeV class energy is 0.018 [electrons/proton] [1], the total SE current becomes several tens of nA. Since the SX beam size is 10 mm, SE current per ribbon is in the nA class. In addition, to achieve sensitivity to halo region as low as approximately three orders of magnitude, an I/V amplifier was designed with sensitivity up to

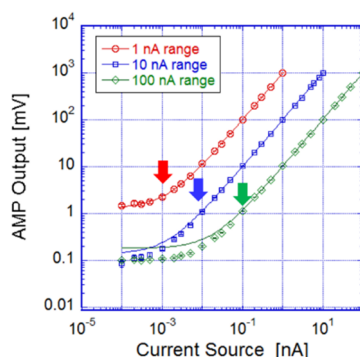


Figure 4: Linearity of I/V amplifier.

pA class. However, on the low sensitivity side, 10 nA and 100 nA classes have also been prepared for larger current of the circulating beam. Considering that the signal path length of 170 m, the input noise of the amplifier becomes a problem. We took a countermeasure to balance with a filter and a limiter of the input section and the capacity of the feedback section of the amplifier. Finally, a 20ch module of I/V circuit made with a hybrid IC configuration was manufactured by Kaizu Works (KB2014A) [4].

Figure 4 shows the linearity of the I/V amplifier with linear fit. The error bars are the standard deviation. The arrow attached to each curve is the applicable lower limit of the straight line. For each range, a dynamic range was approximately  $10^3$ . In the 1 nA [V] range, the straight line is extended to  $10^{-4}$  nA. The deviation from the fitted slope, offset, and response frequency are summarized in Table 1.

### A/D Converter

The continuous voltage output of the 20ch I/V amplifier was real-time averaged for each channel using 12-bit ADCs with a sampling rate of 250MS/s (CAEN V1720 DPP-CI [5]). For the averaging process, using the V1720 FPGA, function of gating and integrating were applied.

## MEASUREMENT OF BEAM PROFILE

Table 1: Range and Characteristics of I/V Amps

Range [nA/V]	Slope Dev. [%]	Offset [%]	Response Frequency [Hz]
100	0.4	0.018	1000
10	0.4	0.013	160
1	0.4	0.13	160

### Beam Profile and Time Structure of Spill

We used 51kW SX beam to test the 20ch simultaneous measurements by SX-MRPM #82. The range of the I/V amplifier was 100 nA /V. In the FPGA, digitized signals were integrated within a gate time of 1.2  $\mu\text{s}$  every 10  $\mu\text{s}$ .

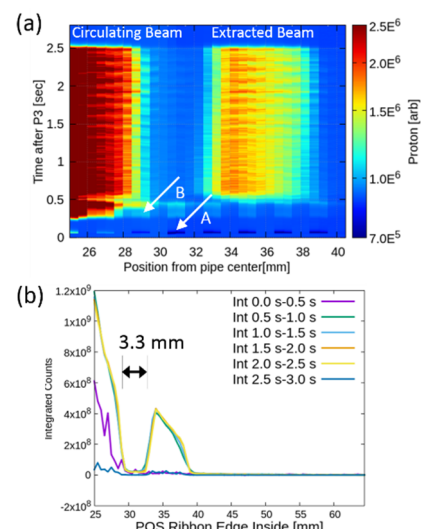


Figure 5: 51 kW-Beam Profile, (a) Log color contour plot, (b) Integrated Profiles at every 500 ms step.

Content from this work may be used under the terms of the CC BY 3.0 licence (© 2019). Any distribution of this work must maintain attribution to the author(s), title of the work, publisher, and DOI

The measurement was done with four steps. First, the edge of the innermost ribbon was set at 25 mm from the central beam orbit. Real-time signal processing was executed during spill time of 2 s by one shot. In the second and subsequent steps, the edge was moved outside by 0.5 mm each time. Then after 4 steps, data for a spatial pitch of 0.5 mm were obtained in a total of 4 shots.

Figure 5 (a) shows the measured beam profile together with the tail of the circulating beam. Also, Figure 5 (b) shows a beam profiles by integrating at time steps of 500 ms. The turn separation of the circulating and the SX beam was 3.3 mm. The size of the SX was approximately 6.5 mm, and was almost constant during the spill time.

Figure 6 shows the time structure of each ribbon. At the 25 mm ribbon edge, evident signal saturation was observed. The circulating beam and the extracted beam both had a periodic small time structure of about 8 Hz. This structure is believed to depend on feedback control in the SX system. Apart from these structures, the spill is almost flat.

### Electron Cloud

An examination of signals A and B in Figs. 5 and 6 reveal that the time zone of A is 0.0 -0.2 s, and that of B is 0.3 - 0.5 s. The data for these time zones were integrated and plotted as shown in Fig.7 (a) and (b). Distinct spikes appeared periodically in both. As previously described, the data were measured in 4 shots with a target movement of 0.5 mm steps. However, both A and B spike signals occurred in only one shot. Figure 7 (a) represents the electron clouds information [6] generated at the time of beam debunching. When the ribbon edge positioned 25 mm, 27 mm, it is a positive signal, and after 29 mm, it is a negative signal. This signal can be seen as far as 65 mm. Since protons do not stop at the ribbon with thickness of 1.1  $\mu\text{m}$ , the spike is considered to be the sum of the charge of the electrons stopped in the ribbon and the emitted SE. Then plus signed represents there are more SE than stopped electrons, and negative signed represents the opposite. Spike signals did not appear in the other three shots, and so they can be read as a beam or electron-cloud that was larger in size than the normal circulating beam.

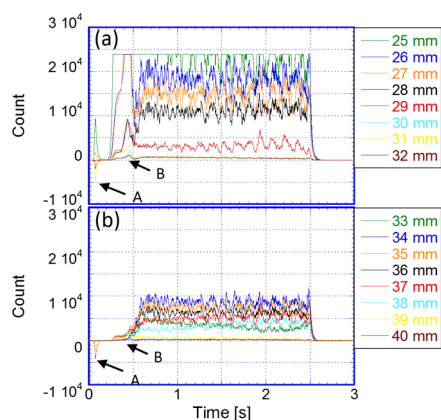


Figure 6: Time structure of each ribbon, (a) Circulating beam, (b) Extracted beam.

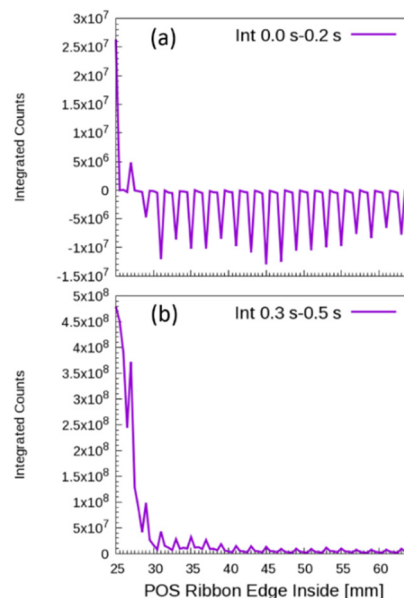


Figure 7: Spatial signal at fixed time region, (a) time 0.0 - 0.2 s, and (b) time 0.3 - 0.5 s.

Figure 7 (b) shows a flying in which the extraction beam was generated earlier than 0.6 s of the spill start time. Given that it occurred in the same shot as Fig. 7 (a) and that the beam spreading occurred in the circulating beam, it was presumed that the electron cloud was attributable.

### CONCLUSION

Using SX-MRPM, evolved multi-graphene ribbons with a thickness of 1.1  $\mu\text{m}$  were arranged in 20 channels with a width of 1 mm and a pitch of 2 mm, profile of the extraction beam could be measured continuously within the spill time. In the measurement system, signal processing was performed with a precise I/V amplifier with a linearity of 1 pA or less for each channel, and its output was processed in real time via gate integration by the FPGA. The information on the electron cloud was a new finding.

### ACKNOWLEDGEMENT

The authors are very grateful to the following individuals: for the fabrication of the target, M. Mitani (MINOTOS), Y. Matsumoto (KOYO SEIKO), and Y. Akao (CITIZEN), for a practical work, we are indebted to S. Otsu, Y. Omori and H. Akino (Mitsubishi Electric System & Service).

### REFERENCES

- [1] Y. Hashimoto *et al.*, "Multi-Ribbon Profile Monitor Using Carbon Graphite Foil for J-PARC", in *Proc. HB'10*, Morschach, Switzerland, Sep.-Oct. 2010, paper WEO2A01, pp. 429-433.
- [2] M. Tomizawa *et al.*, "Status and Beam Power Ramp-Up Plans of the Slow Extraction Operation at J-Parc Main Ring", in *Proc. HB'18*, Daejeon, Korea, Jun. 2018, pp. 347-351. doi:10.18429/JACoW-HB2018-THA1WD03
- [3] AIP Conf. Proc. 1962, 030005 (2018), p.1-6. <https://doi.org/10.1063/1.5035522>
- [4] <http://www.kaizuworks.co.jp/>

- [5] <https://www.caen.it/products/v1720/>
- [6] B. Yee-Rendon *et al.*, “Electron Cloud Simulations for the Main Ring of J-PARC”, in *Proc. IPAC'17*, Copenhagen, Denmark, May 2017, pp. 4436-4438.  
doi:10.18429/JACoW-IPAC2017-THPVA010